

Genus dependence of the number of (non-)orientable surface triangulations

Benedikt Krüger* and Klaus Mecke

FAU Erlangen-Nuremberg, Institute for Theoretical Physics, Staudtstraße 7, 91058 Erlangen, Germany

(Received 27 July 2015; published 13 April 2016)

Topological triangulations of orientable and nonorientable surfaces with arbitrary genus have important applications in quantum geometry, graph theory and statistical physics. However, until now, only the asymptotics for 2-spheres have been known analytically, and exact counts of triangulations are only available for both small genera and triangulations. We apply the Wang-Landau algorithm to calculate the number $N(m, h)$ of triangulations for several orders of magnitude in system size m and type h (equals genus in orientable triangulations). We verify that the limit of the entropy density of triangulations is independent of genus and orientability and are able to determine the next-to-leading-order and the next-to-next-to-leading-order terms. We conjecture for the number of surface triangulations the asymptotic behavior

$$N(m, h) \rightarrow (170.4 \pm 15.1)^h m^{-2(h-1)/5} \left(\frac{256}{27}\right)^{m/2},$$

which might guide a mathematician's proof for the exact asymptotics.

DOI: [10.1103/PhysRevD.93.085018](https://doi.org/10.1103/PhysRevD.93.085018)**I. INTRODUCTION**

Triangulations of manifolds provide a standard method of discretizing surfaces in condensed matter and a possibility for quantizing space-time. They are used in the simplicial quantum gravity models of dynamical triangulations [1] and the causal version thereof [2], as well as in spin foams [3]. Furthermore, they are also a fundamental object within the group field theory approach to quantum gravity [4–6], which can be seen to relate the previously mentioned approaches. For the simplicial quantum geometry models, it is crucial to know the scaling of the number of triangulations in terms of the system size, because on the one hand, the statistical models are only well defined if there exists an exponential scaling, and on the other hand, the scaling constant determines the value of the coupling constant to obtain a phase transition necessary for results independent of the introduced discretization scale [1,2]. Even if triangulations are not seen as a tool for regularization as in simplicial quantum geometry, but as the actual relevant degrees of freedom as in the spin foam or the group field theory approach, the asymptotics of the number of triangulations in terms of the system size is important for the measure term of the path integral.

For rooted triangulations of the 2-sphere, it is well known that their number scales $\propto \sqrt{256/27^m}$, with m being the number of triangles [7]. A triangulation is rooted by marking some vertex as well as some adjacent edge and face as special in order to break symmetry and to simplify the counting procedure. For standard triangulations, the same result was obtained later by proving that the ratio of triangulations possessing any nontrivial symmetry vanishes for large triangulations [8]. For other surfaces with a different

genus or orientability, like the torus or the projective plane, no asymptotic numbers are known, neither for the rooted nor for the default, unrooted case. Nevertheless, for simplicial quantum gravity, triangulations of arbitrary surfaces are important, because the models are not restricted to a certain topology of the underlying manifold.

Triangulations of surfaces with nonvanishing genus are also an object of study in other branches of physics: Since every graph is planar if embedding into a surface with an arbitrary high genus, and triangulations are the maximal planar graphs for the respective surfaces (every insertion of an edge would violate the planarity), they are an important tool in graph and network theory [9–11]. Furthermore, critical properties of statistical systems defined on quantum surfaces or triangulated manifolds are sometimes easier to solve than they would be on Euclidean lattices, but they can be related to these using the KPZ formula [12–14].

Using lexicographic enumeration, it is possible to exactly count triangulations of orientable and nonorientable

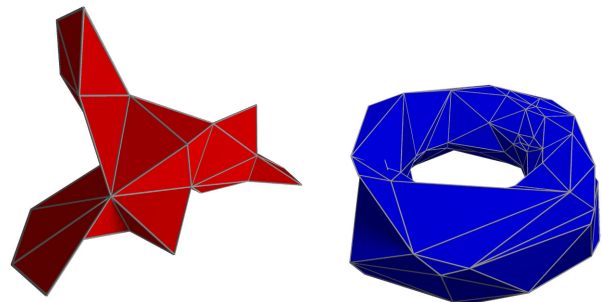


FIG. 1. Examples for triangulations of surfaces with low genera. (Left, red): Triangulation of the 2-sphere with $m = 50$ maximal simplices. (Right, blue): Triangulation of the torus (orientable surface with genus $g = 1$) with $m = 200$ maximal simplices.

*benedikt.krueger@fau.de

surfaces for small genera $g \leq 6$ and a small number of vertices $v \leq 23$ [15–17]. For bigger genera or larger triangulations, this method does not give results in any reasonable computation time.

In contrast to triangulations, the asymptotic behavior of (triangular) maps on surfaces is far better understood. A triangular map is a graph drawn on a surface so that each face is a triangle; the main difference from triangulations is that triangular maps allow for digons, multiple edges or loops. One can show that the asymptotic number $T(k, h)$ (orientable) and $P(k, h)$ (nonorientable) of certain classes of maps on arbitrary surfaces has the form [18]

$$\begin{bmatrix} T(k, h) \\ P(k, h) \end{bmatrix} = \alpha \begin{bmatrix} t_h \\ p_h \end{bmatrix} (\beta k)^{5(h-1)/2} \cdot \gamma^k, \quad (1)$$

where k is the number of edges and $h = g$ (orientable) or $h = g/2$ (nonorientable) is the type of the surface. The constants t_h and p_h only depend on h and not on the class of maps that are counted; they were calculated in Ref. [19] using a recursion relation obtained in Ref. [20]. The numbers α , β and γ depend on the class of surface; one finds e.g. $\gamma = 12$ for all maps [21] or $\gamma = 2^{2/3}\sqrt{3}$ for triangular maps [22].

In this paper we numerically approximate the number of surface triangulations in terms of the genus g and the number of triangles m using the Wang-Landau algorithm [23,24] for several orders of magnitude in g and m . A similar version of this method was used in Ref. [25] to approximate the number of lattice triangulations. We are able to extract the long-sought asymptotics for the number of triangulations of arbitrary surfaces for the first time and find an exponential growth that coincides with the one found for spheres in Ref. [8]. Additionally, we determine the subexponential corrections similar to Eq. (1), which are a valuable hint for mathematicians proving the exact asymptotics for the number of surface triangulations. The presented method is not limited to estimating the total number of surface triangulations, but it can also be used for estimating the asymptotics of the cardinality for certain subclasses of these triangulations. A possible application can be estimating the asymptotic number of irreducible triangulations, which are triangulations without contractible edges (see Ref. [26] for a detailed definition, and Ref. [15] for enumerations of small irreducible triangulations). Furthermore, our method can also be applied to k -equivelar or k -covered triangulations, where in the former every vertex has degree k and in the latter there is at least one vertex with degree k (see Refs. [27,28] for detailed discussion and numbers for few vertices), and to many more different subclasses of triangulations.

II. CONSTRUCTION OF TRIANGULATIONS

First, we present the definition of triangulations of (closed) surfaces M by using the notion of simplicial

complexes. Let \mathcal{I} be a set and $K \subset 2^{\mathcal{I}}$ a set of subsets of \mathcal{I} . K is an *abstract simplicial complex* if it is complete ($\sigma \in K, \sigma' \subset \sigma \Rightarrow \sigma' \in K$) and closed under the formation of intersections ($\sigma_1, \sigma_2 \in K \Rightarrow \sigma_1 \cap \sigma_2 \in K$). A *triangulation* \mathcal{T} of the two-dimensional surface M is an abstract simplicial complex K equipped with a geometric realization (coordinization of every element of \mathcal{I}) that is homeomorphic to M . Since the topology of a closed surface is determined only by its Euler characteristic, or equivalently by its genus and orientability [29], this is also true for the topology of their triangulations. Two examples for surface triangulations can be found in Fig. 1.

Triangulations of orientable and nonorientable surfaces with arbitrary genus $g \neq 0$ can be constructed in terms of an arbitrary triangulation of the torus \mathbb{T} (orientable surface with $g = 1$) or the projective plane \mathbb{P} (nonorientable surface with $g = 1$), using the connected sum $\#$. Triangulations of the torus and the projective plane can be found e.g. in Ref. [30]. The connected sum of two triangulated surfaces is created easily by removing a triangle from each triangulation and gluing the boundary together. A (non-)orientable surface with genus g can then be constructed by taking the g -fold connected sum $\mathbb{T}\#\mathbb{T}\#\dots\#\mathbb{T}$ ($\mathbb{P}\#\mathbb{P}\#\dots\#\mathbb{P}$) of the torus (projective plane). A triangulation of the 2-sphere, which is the orientable surface with $g = 0$, is given by the boundary of a 3-simplex.

In order to create all possible triangulations of a surface M with given genus and orientability, we introduce some elementary steps called *Pachner moves* [31] (which are modification of Alexander moves [32]) that preserve the topology of the underlying manifold M and allow us to ergodically create every triangulation of M from every other triangulation of M . In two dimensions, there are three different Pachner moves (see Fig. 2): The first inserts a vertex into a triangle (insertion move), its inverse step removes a three-valent vertex from the triangulation (removal move). The third step replaces one diagonal of a quadrangle with the other triangle (diagonal-edge move) and is its own inverse. In two dimensions, the diagonal-edge moves are ergodic for the subset of triangulations with the same number of vertices v , if one chooses a large enough v [33,34].

In order to construct a triangulation of a orientable or nonorientable surface of a given genus g and given number of vertices v or number of triangles m , we first create a triangulation with the proper genus by taking the connected sum of tori or projected planes as described above. If the number of triangles in this triangulation is smaller than m ,



FIG. 2. Elementary Pachner moves in two dimensions. (Left): Insertion and removal of a vertex. (Right): Diagonal-edge flip, which is ergodic in the subset of triangulations with the same number of vertices.

we perform insertion moves until the number of vertices equals m . If, otherwise, the number of triangles is bigger than m , we perform removal moves until the triangulation is small enough, and in between diagonal-edge moves if no removal move is possible. Note that there is a lower bound on the number of vertices or triangles necessary to triangulate a surface with given genus [35–37], so it is not possible to create arbitrary small triangulations for a given g .

III. NUMERICAL COUNTING ALGORITHM

We use the Wang-Landau Markov-chain Monte Carlo algorithm [23,24] to numerically measure the density of states (DOS) $g(m)$, which is up to a normalization factor the number of triangulations with m triangles. In general, a Markov-chain Monte Carlo algorithm generates samples $\omega \in \Omega$ from a sample space Ω according to a given probability distribution $P(\omega)$ by creating a Markov chain of samples with stationary distribution $P(\omega)$. Therefore, the transition probabilities $P(\omega \rightarrow \omega')$ have to fulfill the detailed balance condition

$$\frac{P(\omega_1 \rightarrow \omega_2)}{P(\omega_2 \rightarrow \omega_1)} = \frac{P(\omega_2)}{P(\omega_1)}. \quad (2)$$

A famous and often-used example is the Metropolis algorithm [38], where $P(\omega) \propto \exp[-\beta E(\omega)]$ is basically the Boltzmann factor. The Wang-Landau algorithm uses the probability distribution

$$P_{\text{WL}}(\omega) = \frac{1}{g(E(\omega))} \quad (3)$$

so that the probability distribution in terms of the energies is flat, and chooses the transition probabilities

$$P(\omega_1 \rightarrow \omega_2) = \min \left(1, \frac{g(E(\omega_1))}{g(E(\omega_2))} \right). \quad (4)$$

For the considered system of triangulations, we use as the energy of a triangulation \mathcal{T} its number of triangles m , so that every number m of triangles is sampled equally often.

Naturally, the DOS is a prior unknown, as in most physical problems; otherwise the problem of counting the triangulations would already be solved. So the Wang-Landau algorithm takes an initial estimation of the DOS (in our case, a flat distribution $g_{\text{initial}} \propto 1$) and improves it gradually by $g(m) \rightarrow f \cdot g(m)$ whenever a state with m triangles occurs in the Markov chain. Here $f > 1$ is a modification factor that decreases during the simulation whenever the histogram of visited energies $H(m)$ recorded at this modification factor is approximately flat to ensure the DOS anneals to the correct DOS. We use $f \rightarrow f^{0.9}$ as the decrease for the modification factor, and consider the histogram of visited energies to be flat if

$\min[H(m)] \geq c \cdot \text{avg}[H(m)]$ with $c = 0.99$ at the beginning of the simulation, relaxing this condition to $c = 0.8$ with decreasing modification factor. [Note that $H(E)$ is reset after each decrease of the modification factor.] Our first modification factor is $f = \exp(1)$ and decreases to $f = \exp(10^{-8})$ during the simulation. Our choice of parameters is much more careful than the original parameters proposed in Refs. [23,24], resulting in a very small statistical error for our results.

Instead of counting the number $N_t(m, g)$ of triangulations, we calculate the entropy density $\kappa_c(m, g)$ defined by

$$\kappa_c(m, g) := m^{-1} \log N_t(m, g). \quad (5)$$

By using the entropy density, we can use directly the output of the Wang-Landau algorithm, which is for numerical reasons the logarithm DOS, and cancel the normalization factor. It is also a common quantity discussed in the literature [25,39,40] and corresponds to the value of the (causal) dynamical triangulations' coupling constant for obtaining scale invariance [1,2]. In Fig. 3, a comparison between our calculations and results obtained by lexicographic enumeration for small triangulations [17] shows excellent agreement and justifies our method.

Due to the diagonal-edge flips being ergodic for large enough surface triangulations, it is sufficient to calculate the density of states in an interval $[m - 2, m + 2]$ to obtain the entropy density κ_c by

$$\kappa_c(m) = \frac{1}{8} \cdot \log \frac{g(m+2)}{g(m-2)}, \quad (6)$$

using the assumption that $\kappa_c(m \pm 2) \approx \kappa_c(m)$ valid for large m . Choosing this small interval of computation, the calculation speeds up drastically compared to determining

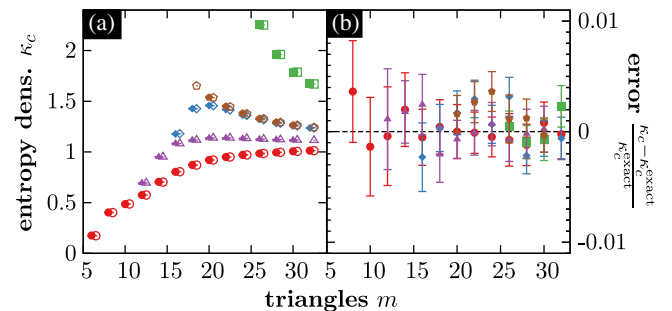


FIG. 3. Comparison of the exact entropy density from Ref. [17] and our numerical calculations. (a) Entropy density $\kappa_c(m, g)$ in terms of the number of triangles m for orientable surfaces ($g = 0$: red circles, $g = 1$: blue diamonds, $g = 2$: green squares) and nonorientable surfaces ($g = 1$: purple triangles, $g = 2$: brown pentagons). Our numerical data is plotted with filled symbols; the exact values are plotted with empty symbols and are shifted slightly to the right to resolve these points. (b) Relative error $\kappa_c(m, g)/\kappa_c^{\text{exact}}(m, g) - 1$ of the numerical data with respect to the exact values.

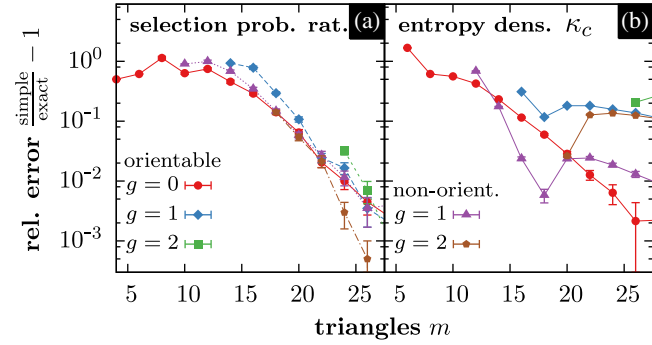


FIG. 4. Influence of using the simplified selection probability, not taking into account isomorphism. (a) Relative error of the selection probability factors for orientable ($g=0$: red circles, $g=1$: blue diamonds, $g=2$: green squares) and nonorientable ($g=1$: purple triangles, $g=2$: brown pentagons) surfaces in terms of the number of triangles. (b) Relative error of the entropy density.

the whole DOS using the Wang-Landau algorithm, because computation time scales with the number of bins.

In order to fulfill the detailed balance condition in the Wang-Landau algorithm and to correctly calculate the transition probabilities, one has to compute for each flip the ratio of the selection probabilities of the flip and those of the inverse flip. Assuming that the triangulation has no special symmetries, the selection probabilities can be determined in terms of the current simplex numbers and their change induced by the flip. However, there are symmetric triangulations which make it necessary to check whether there are other flips leading to an isomorphic triangulation (these flips are then equivalent), and the same for the inverse flip. These isomorphism checks increase drastically the computation time needed for one step. But fortunately, as depicted in Fig. 4, the deviations of the exact (with isomorphisms) calculated and the simplified calculations are negligible for triangulations with $m > 30$. These results are comparable with those of Ref. [41] on the level of maps, where it was shown that almost all maps do not possess intrinsic symmetries, which implies in our notion that the simplified and exact selection probabilities match.

IV. RESULTS

We calculated the entropy density (6) $\kappa_c(m, g)$ for orientable and nonorientable surface triangulations up to genus $g_{\max} = 1000$ and up to $m_{\max} = 10^7$ triangles using 400 independent Wang-Landau simulations each. In Figs. 5 and 6 $\kappa_c(m, g)$ is displayed for fixed genus and for fixed number of triangles.

Inspired by the asymptotic enumeration results for triangulations of the 2-sphere and for maps on arbitrary surfaces, we assume that the number of triangulations behaves as

$$N(m, g) = \bar{a}(g) \cdot \bar{b}(g)^m \cdot m^{\kappa_c^\infty(g)}. \quad (7)$$

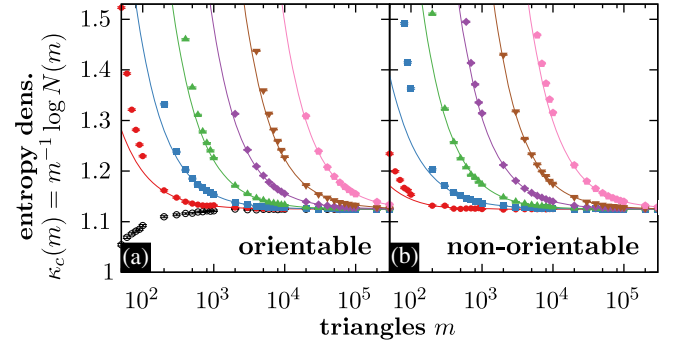


FIG. 5. Entropy density for triangulations of orientable (a) and nonorientable (b) surfaces in terms of the number of triangles m for the genera $g=0$ (black, unfilled circles) (only orientable), $g=3$ (red, filled circles), $g=10$ (blue squares), $g=30$ (green, up-pointing triangles), $g=100$ (purple diamonds), $g=300$ (brown, down-pointing triangles) and $g=1000$ (pink pentagons). The lines are fits of Eq. (8) with respect to $a(g)$ and $b(g)$.

This implies for the entropy density (6) the relation

$$\kappa_c(m, g) = a(g) \cdot \frac{1}{m} + b(g) \cdot \frac{\log(m)}{m} + \kappa_c^\infty(g). \quad (8)$$

Considering Fig. 5, we find that the constant term $\kappa_c^\infty(g)$ in Eq. (8) does not depend on the genus g or on whether the surface is orientable; furthermore, we find excellent agreement with the theoretical value of $\log(\sqrt{256/27}) \approx 1.1247$ obtained for triangulations of the sphere [8]. By inspecting $\kappa_c(m, g=1)$, one finds that for $g=1$ the entropy density is approximately constant in terms of m , which implies that $b(g) \propto b_1 \cdot (g-1)$ without any constant term, in agreement with Refs. [8] and [19], where $b_1 = 7/2$ for triangulations of the 2-sphere and $b_1 = 5/2$ for triangular maps on surfaces.

To obtain the constants $a(g)$ and $b(g)$, we rescale the entropy density (8) so that

$$m \cdot [\kappa_c(m, g) - \kappa_c^\infty(g)] = a(g) + b(g) \log m.$$

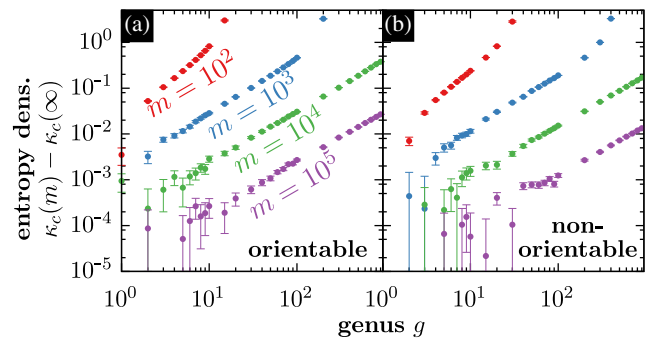


FIG. 6. Deviation of the entropy density from the limiting value κ_c^∞ for triangulations of (a) orientable and (b) nonorientable surfaces in terms of the genus g for $m=10^2$ (red), $m=10^3$ (blue), $m=10^4$ (green), and $m=10^5$ (purple) triangles.

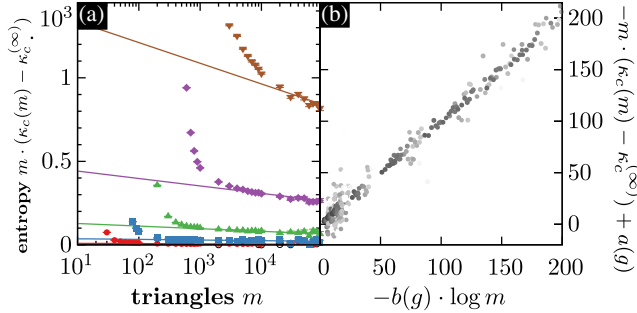


FIG. 7. Scaling of the entropy density. (a) Plot of the entropy $m \cdot \kappa_c(m)$ in terms of the logarithm of the number m of triangles used to extract the constants $a(g)$ and $b(g)$ by fitting a straight line. The data points are the same as those used in Fig. 5. (b) Collapse of the data points; the points are darker for smaller error, and only points with $\kappa_c(m)/\kappa_c^\infty < 1.05$ are plotted.

For every genus g , both constants can then be determined by a linear fit of the rescaled entropy density in terms of $\log m$. In Fig. 7(a), the rescaled entropy density is plotted for orientable surfaces of different genera; one can see an excellent agreement with the proposed linear dependency in terms of $\log m$ for sufficient triangles. Using the fitted constants, all obtained data points can be brought to collapse as depicted in Fig. 7(b).

Having fitted $a(g)$ and $b(g)$ for all considered genera of orientable and nonorientable surfaces, one can access numerically the scaling relation of both constants for triangulations as depicted in Fig. 8. The leading order $b(g) = b_1 \cdot (g - 1)$ does differ from the results for triangular maps qualitatively; we find $b_1 = -0.197 \pm 0.006$ for orientable and $b_1 = -0.102 \pm 0.004$ for nonorientable triangulations, while for triangular maps the theoretical value $b_1 = 5/2$ was found [19]. We conjecture that $b_1 = -2/5$ for orientable and $b_1 = -1/5$ for nonorientable surface triangulations, since these small integer fractions are in the 1σ bounds of the numerically obtained values. The next-to-leading order $a(g) = (5.14 \pm 0.09) \cdot g$ (orientable) and $a(g) = (2.60 \pm 0.03) \cdot g$ (nonorientable) has a linear dependency on g for the considered range of genera

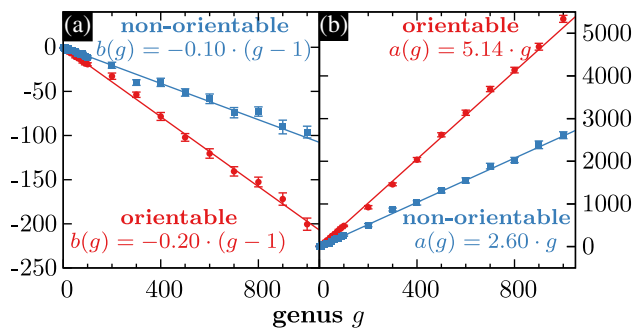


FIG. 8. Values of the asymptotic constants a and b in terms of the genus g for orientable (red circles) and nonorientable (blue squares) triangulations. The corresponding lines are linear fits.

[implying $\bar{a} \propto \exp(g)$ in Eq. (7)]; no logarithmic correction as proposed in Ref. [19] for triangular maps is present. For both $a(g)$ and $b(g)$, one can deduce that the results for orientable and nonorientable triangulations coincide if one does not consider the genus, but the type of the surface (which is half the genus for non-orientable surfaces).

V. CONCLUSION AND OUTLOOK

In this paper, the number of triangulations of (orientable and nonorientable) surface triangulations with arbitrary genus was calculated using the Wang-Landau Markov-chain Monte Carlo algorithm. Based on our results, we conjecture the following relation for the asymptotic number of surface triangulations:

$$N(m, h) \rightarrow (170.4 \pm 15.1)^h m^{-2(h-1)/5} \left(\frac{256}{27}\right)^{m/2}, \quad (9)$$

in terms of the type h of the surface, which equals the genus g for orientable and half its value for nonorientable triangulations.

These quantitative results for the leading- and next-to-leading-order terms can be a valuable hint for mathematicians proving the exact asymptotics of the number of surface triangulations. Additionally, the numerical method presented in this paper can be directly applied to estimate the number and its asymptotics of special types of triangulations, e.g. irreducible, k -equivelar or k -covered triangulations.

Using the presented method makes it possible to find the scaling behavior of triangulations of higher-dimensional manifolds (either of the total number or of the number of triangulations with certain properties), and to conjecture about fundamental questions that could not be answered until now. For example, the question of whether there are exponentially many or more triangulations of the d -sphere (or another underlying manifold) in terms of the number of maximal simplices (facets) [42] can only be answered for certain subclasses of triangulations (e.g., locally constructable triangulations [43,44], geometric triangulations [45], triangulations with a Morse function with a fixed number of critical cells [46], or melonic triangulations, which are the dominant contribution to the $1/N$ expansion in group field theory [47]), the answer is there are more than exponentially many in terms of the number of vertices for d -spheres [48–50]. However, in three or more dimensions, the computational effort increases due to the fact that for each data point one has to calculate the DOS $g(m)$ for a much larger interval in the number m of maximal simplices to ensure ergodicity, since there is no similar result as in Refs. [33,34].

Our methods and results can also be used for solving simplicial quantum gravity models like (causal) dynamical triangulations on surfaces with arbitrary genus, where the

leading-order term gives the value of the coupling constant necessary for obtaining scale-independent limits. Furthermore, the next-to-leading-order terms can provide insights into their finite size scaling, which is important, since these models are solved mainly using Monte Carlo simulations.

ACKNOWLEDGMENTS

The authors thank J. F. Knauf for fruitful discussions, as well as B. Benedetti for calling our attention to Ref. [50]. This work is supported by EFI Quantum Geometry and the Elite Network of Bavaria.

-
- [1] J. Ambjørn, *Classical Quantum Gravity* **12**, 2079 (1995).
 [2] J. Ambjørn, J. Jurkiewicz, and R. Loll, *Phys. Rev. D* **72**, 064014 (2005).
 [3] C. Rovelli, *Quantum Gravity*, Cambridge Monographs on Mathematical Physics (Cambridge University Press, Cambridge, England, 2007).
 [4] L. Freidel, *Int. J. Theor. Phys.* **44**, 1769 (2005).
 [5] D. Oriti, in *Foundations of Space and Time. Reflections on Quantum Gravity*, edited by J. Murugan, A. Weltmann, and G. F. R. Ellis (Cambridge University Press, Cambridge, England, 2012) pp. 257–320.
 [6] V. Rivasseau, *AIP Conf. Proc.* **1444**, 18 (2012).
 [7] W. T. Tutte, *Can. J. Math.* **14**, 21 (1962).
 [8] W. T. Tutte, *J. Comb. Theory B* **28**, 105 (1980).
 [9] J.-P. Kownacki, *Eur. Phys. J. B* **38**, 485 (2004).
 [10] J. S. Andrade, H. J. Herrmann, R. F. S. Andrade, and L. R. da Silva, *Phys. Rev. Lett.* **94**, 018702 (2005).
 [11] T. Aste, R. Gramatica, and T. Di Matteo, *Phys. Rev. E* **86**, 036109 (2012).
 [12] V. G. Knizhnik, A. M. Polyakov, and A. B. Zamolodchikov, *Mod. Phys. Lett. A* **03**, 819 (1988).
 [13] B. Duplantier and S. Sheffield, *Invent. Math.* **185**, 333 (2011).
 [14] C. Garban, *Asterisque* **352**, 1052 (2013).
 [15] T. Sulanke, <http://hep.physics.indiana.edu/~tsulanke/graphs/surftri/counts.txt>.
 [16] G. Brinkmann and B. D. McKay, *Commun. Math. Comput. Chem.* **58**, 323 (2007).
 [17] T. Sulanke and F. H. Lutz, *Eur. J. Combin.* **30**, 1965 (2009).
 [18] Z. Gao, *J. Comb. Theory A* **64**, 246 (1993).
 [19] E. A. Bender, Z. Gao, and L. B. Richmond, *Electron. J. Comb.* **15**, R51 (2008).
 [20] I. P. Goulden and D. Jackson, *Adv. Math.* **219**, 932 (2008).
 [21] E. A. Bender and E. R. Canfield, *J. Comb. Theory A* **43**, 244 (1986).
 [22] Z. Gao, *J. Comb. Theory B* **52**, 236 (1991).
 [23] F. Wang and D. P. Landau, *Phys. Rev. Lett.* **86**, 2050 (2001).
 [24] F. Wang and D. P. Landau, *Phys. Rev. E* **64**, 056101 (2001).
 [25] J. F. Knauf, B. Krüger, and K. Mecke, *Europhys. Lett.* **109**, 40011 (2015).
 [26] D. Barnette and A. Edelson, *Isr. J. Math.* **67**, 123 (1989).
 [27] S. Negami and A. Nakamoto, *Graphs Combin.* **17**, 529 (2001).
 [28] F. H. Lutz, T. Sulanke, A. K. Tiwari, and A. K. Upadhyay, [arXiv:1001.2777](https://arxiv.org/abs/1001.2777).
 [29] H. R. Brahana, *Ann. Math.* **23**, 144 (1921).
 [30] F. H. Lutz, <http://page.math.tu-berlin.de/~lutz/stellar/>.
 [31] U. Pachner, *Abh. Math. Sem. Univ. Hamburg* **57**, 69 (1986).
 [32] J. W. Alexander, *Ann. Math.* **31**, 292 (1930).
 [33] S. Negami, *Discrete Math.* **135**, 225 (1994).
 [34] S. A. King, *Topol. Appl.* **127**, 169 (2003).
 [35] P. Heawood, *Quart. J. Pure Appl. Math.* **24**, 332 (1890).
 [36] G. Ringel, *Math. Ann.* **130**, 317 (1955).
 [37] M. Jungerman and G. Ringel, *Acta Math.* **145**, 121 (1980).
 [38] N. Metropolis, A. W. Rosenbluth, M. N. Rosenbluth, A. H. Teller, and E. Teller, *J. Chem. Phys.* **21**, 1087 (1953).
 [39] S. Catterall, J. Kogut, and R. Renken, *Phys. Lett. B* **342**, 53 (1995).
 [40] V. Kaibel and G. M. Ziegler, in *Surveys in Combinatorics 2003*, Lond. Math. Soc. Lect. Note Ser. 307 (Cambridge University Press, Cambridge, England, 2003), pp. 277–308.
 [41] L. Richmond and N. Wormald, *J. Comb. Theory B* **63**, 1 (1995).
 [42] M. Gromov, in *Visions in Mathematics*, Modern Birkhäuser Classics, edited by N. Alon, J. Bourgain, A. Connes, M. Gromov, and V. Milman (Birkhäuser Basel, Berlin, 2010), pp. 118–161.
 [43] B. Durhuus and T. Jonsson, *Nucl. Phys.* **B445**, 182 (1995).
 [44] B. Benedetti and G. M. Ziegler, *Acta Math.* **206**, 205 (2011).
 [45] K. Adiprasito and B. Benedetti, [arXiv:1107.5789](https://arxiv.org/abs/1107.5789).
 [46] B. Benedetti, *Trans. Am. Math. Soc.* **364**, 6631 (2012).
 [47] R. Gurau and J. P. Ryan, *SIGMA* **8**, 020 (2012).
 [48] G. Kalai, *Discrete Comput. Geom.* **3**, 1 (1988).
 [49] J. Pfeifle and G. M. Ziegler, *Math. Ann.* **330**, 829 (2004).
 [50] E. Nevo, F. Santos, and S. Wilson, *Math. Ann.* **364**, 737 (2016).